Supporting information

Visible light driven (VLD) reduced TiO_{2-x}nanocatalysts designed by inorganic and organic reducing agents mediated solvothermal methods for electrocatalytic and photocatalytic applications

Sadaf Jamil[a], Naila Jabeen[b]*, Fatima Sajid[a], Latif U. Khan[c],Afia Kanwal[a], Manzar Sohail[d], Muhammad Zaheer[e],Zareen Akhter[a]*

Authors Affiliation:

[a] Department of chemistry, Quaid-i-Azam university Islamabad 45320, Pakistan

[b] Nanosciences and Technology Division, National Centre for Physics, QAU Campus, Shahdra Valley Road, P.O. Box 2141, Islamabad-44000, Pakistan

[c] Synchrotron-light for Experimental Science and Applications in the Middle East (SESAME) P.O. Box 7, Allan 19252, Jordan

[d] School of Natural Sciences, National University of Sciences and Technology (NUST), H-12, Islamabad, Pakistan

[e] Lahore University of Management Sciences DHA, Lahore cantt, 54792, Pakistan

Corresponding Authors:

Dr Naila Jabeen

Naila.jabeen@ncp.edu.pk

Naila.chem@gmail.com

Prof. Dr Zareen Akhter

zareen_a@qau.edu.pk

S.i. XAFS spectra measurements and fitting

The X-ray absorption fine structure (XAFS) spectra were measured on the XAFS/XRF beamline, Synchrotron-Light for Experimental Science and Applications in the Middle East (SESAME), operating at 2.5 GeV in "decay" mode with a maximum electron current of 250 mA. XAFS spectra were acquired in fluorescence mode with a Silicon Drift Detectors (SDD), KETEK GmbH at room temperature, in the spectral range of Zn K-edge (9659 eV) for the Z-C-TiO_2 and Z-R-TiO_{2-x}. X-ray beam intensity before and after the sample was also measured by two ionization chambers filled with a mixture of noble gases. The energy was calibrated according to the absorption *K*-edge of Zn metallic foil. The samples were prepared in pallet form by pressing a homogeneous mixture of calculated quantity of finely ground material and polyvinylpyrrolidone (PVP) powder. The amount of material in each pellet was calculated using XAFS mass software to give an absorption μ_t~1.5, just above the Zn absorption K-edge.

The extended X-ray absorption fine structure (EXAFS) spectra were quantitatively analyzed and nonlinear best fit was performed for the Fourier transformed k^2-weighted experimental EXAFS signals, using Artemis program [1] from the Demeter. The EXAFS data were preprocessed in Athena. Fitting procedure employs both the imaginary and real parts of the Fourier transformed EXAFS oscillations and theoretical EXAFS paths that were constructed from the ZnSe zinc-blende structure of lattice parameters (a = 5.674, b = 5.674 and c = 5.674 Å) using FEFF 8-lite code in Artemis program. The best fits to the Zn *K*-edge EXAFS data were performed in R-space in the interval of 1–4.0 Å with Hanning windows in the 3-12 $Å^{-1}k$ range, and two single scattering (SS) paths were used, including Zn-Se (2.45 Å) and Zn-Zn (4.00 Å).

The fitting parameters included amplitude reduction factor (S_0^2) and correction to the difference in photoelectron energy between the experimental data and FEFF calculation (ΔE), which were set similar for all the scattering paths. Whereas, interatomic distances (R) and disorder in the bond lengths or mean-square relative displacements (MSRDs), also known as Debye-Waller factors (σ^2) were refined to get the best fit result.

S.ii. Electrochemical studies

The electrochemical studies were conducted on an electrochemical workstation (CHI 660D) in a standard three-electrode system with the as-prepared electrocatalysts on fluorine-doped tin oxide (FTO) glasses as the working electrode, a Pt wire as the counter electrode and Ag/AgCl as the reference electrode. The electrolyte was an aqueous solution of 0.1 M NaOH (pH = 13). The working electrode was fabricated as follows: 300 mg of active material was sonicated with absolute ethanol and nafion to form slurry, following by coating the slurry on a piece of FTO glass.

The measured potentials vs. Ag/AgCl were converted to the reversible hydrogen electrode (RHE) scale according to the Nernst equation [2] given below:

$$E_{RHE} = E_{Ag/AgCl} + 0.059pH + E_{Ag/AgCl}^{0} \quad \text{(S. i)}$$

Where E_{RHE} is the converted potential vs. RHE, $E_{Ag/AgCl}$ is the experimental potential measured against Ag/AgCl reference electrode, and $E^{o}_{Ag/AgCl}$ is the standard potential of Ag/AgCl at 25 ^{o}C (0.1976 V). LSV (OER & HER) were performed at scan rate of 50 mV/ s. The CV was done at scan rate of 25 mV/ s, 50 mV/ s, 100 mV/ s, 200 mV / s, 400 mV / s and 800 mV / s. EIS measurements were done at a frequency of 0.1- 100000 Hz.

S.iii. Photocatalytic activity evaluation

The application of synthesized photocatalysts was investigated by photodegradation of the reactive blue-866 (RB-866) dye under visible light irradiation in sunlight. Photocatalytic activity was tested by mixing 5 mg of the photocatalysts (C-TiO_2, Z-C-TiO_2, R-TiO_{2-x} and Z-R-TiO_{2-x}) (1 g/L) in 50 mL of reactive blue-866 dye solution (20 ppm prepared in double distilled water). After ultrasonication, the samples were bubbled with atmospheric oxygen for about 1hour in order to create adsorption desorption equilibrium. After dark adsorption period, the first sample was taken out considered as initial concentration. Five more samples were regularly withdrawn from the reactor after 10, 20, 30, 40 and 50 min of direct sunlight irradiation. These solutions were immediately centrifuged to separate any suspended solids and analyzed using a UV-Vis spectrophotometer to measure the percentage degradation at wavelength range of 350 nm - 750 nm. The following equation was used to find out the percent degradation activity of each photocatalyst [3].

$$\eta(\%) = \frac{A_0 - A_t}{A_0} \times 100 \qquad \text{(S. ii)}$$

Where A_o = initial concentration of dye, A_t = concentration of dye at time t.

S.iv. Theoratical band edge calculation

Butler and Ginley introduced a theoretical approach [4] for the prediction of the position of band edges using the above relation where E_0 is the energy of free electrons on the hydrogen scale (4.44 ± 0.02 eV), E_g is the band gap energy, and χ is the Sanderson electro negativity of the semiconductor, expressed as the geometric mean of the electro negativities of

the constituent atoms, which are defined after Mulliken as the arithmetic mean of the atomic electron affinity and the first ionization energy (both in eV). Equations S. (iii,iv) are given below

$$E_{VB} = \chi - E_0 + 0.5E_g \quad \text{(S.iii)}$$

$$E_{CB} = E_{VB} - E_g \quad \text{(S. iv)}$$

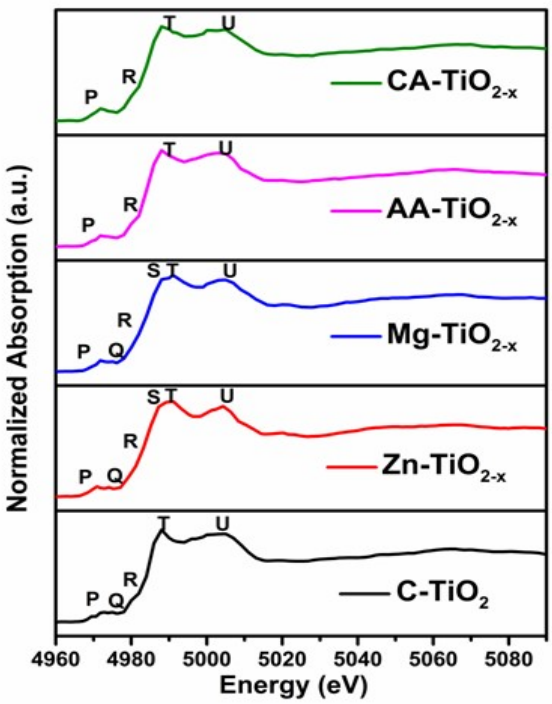

Figure S.1 : Ti *K*-edge (4966 eV) X-ray absorption near edge structure (XANES) spectra of (C-TiO_2), Mg-TiO_{2-x}, CA-TiO_{2-x}, AA-TiO_{2-x} and Zn-TiO_{2-x}

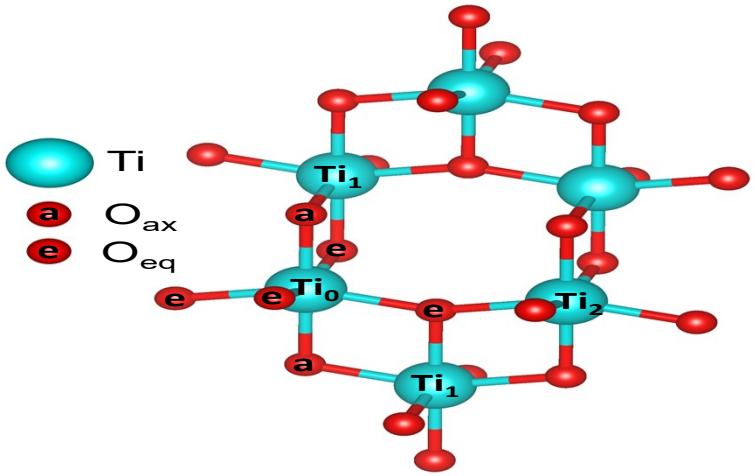

Figure S.2: 3D structure of anatase titania

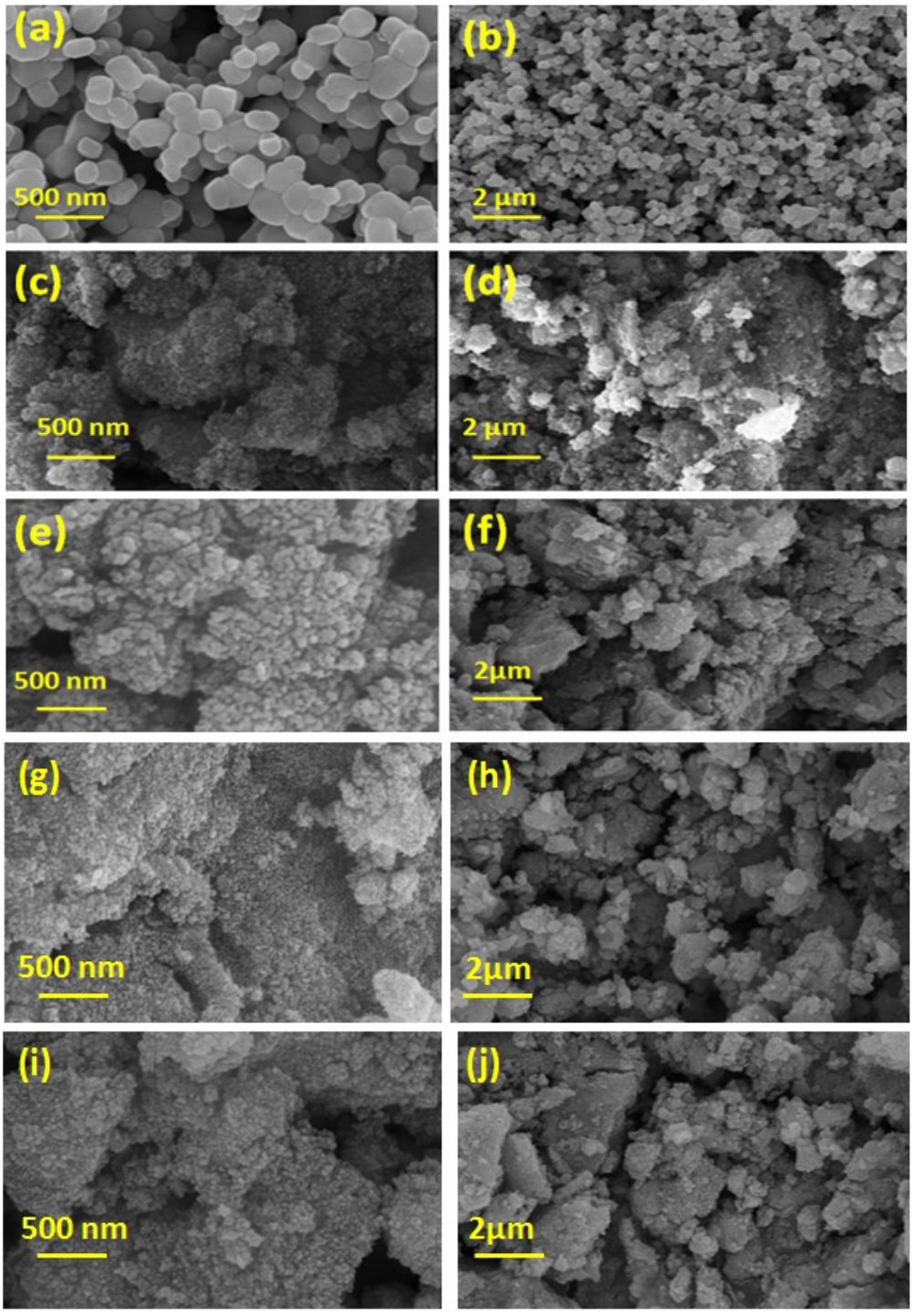

Figure S.3: SEM micrographs of (a,b) C-TiO_2, (c,d) Zn-TiO_{2-x}, (e,f) Mg-TiO_{2-x}, (g,h) AA-TiO_{2-x} and (i,j) CA-TiO_{2-x} nanocatalysts.

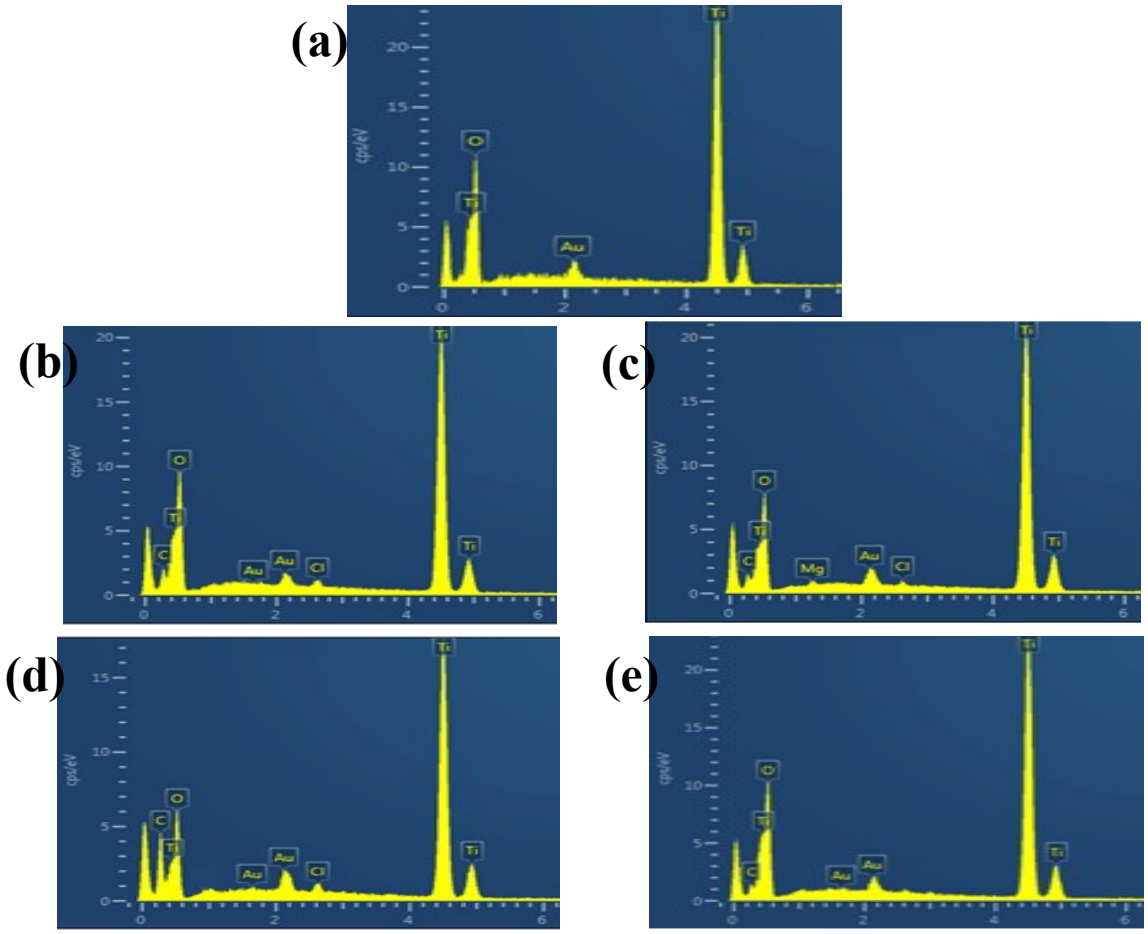

Figure S.4: EDS spectra of (a) C-TiO_2, (b) Zn-TiO_{2-x}, (c) Mg-TiO_{2-x}, (d) AA-TiO_{2-x} and (e) CA-TiO_{2-x} nanocatalysts.

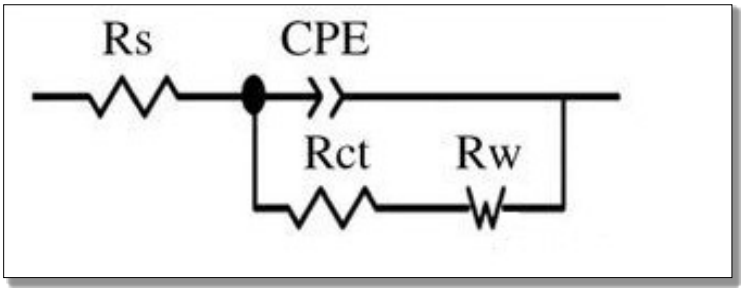

Figure S.5: Equivalent circuit for CPE model.

Material	Bond Type	N	R(Å)
C-TiO_2	Ti_0-O_{eq}	3.9	1.912±0.0101
	Ti_0-O_{ax}	1.9	1.960±0.0101
	Ti_0-Ti_1	4	3.067±0.0148
	Ti_0-Ti_2	3.9	3.749±0.0371
Zn-TiO_{2-x}	Ti_0-O_{eq}	3.9	1.907±0.0196
	Ti_0-O_{ax}	1.7	2.034±0.0449
	Ti_0-Ti_1	3.3	3.060±0.0235
	Ti_0-Ti_2	2.8	3.652±0.1488
Mg-TiO_{2-x}	Ti_0-O_{eq}	3.7	1.911±0.0287
	Ti_0-O_{ax}	1.9	1.992±0.0499
	Ti_0-Ti_1	3.5	3.068±0.0189
	Ti_0-Ti_2	2.7	3.663±0.240
AA-TiO_{2-x}	Ti_0-O_{eq}	3.9	1.913±0.0112
	Ti_0-O_{ax}	1.7	1.961±0.0112
	Ti_0-Ti_1	4	3.068±0.0190
	Ti_0-Ti_2	3.7	3.727±0.0551
CA-TiO_{2-x}	Ti_0-O_{eq}	3.5	1.921±0.0101
	Ti_0-O_{ax}	1.3	1.969±0.0101
	Ti_0-Ti_1	4	3.084±0.0173
	Ti_0-Ti_2	3.9	3.733±0.0526

Table S.1. Derived EXAFS fitting parameters, including N: coordination number, R: mean coordination shell radii, σ^2: mean square relative displacements (MSRDs) or Debye–Waller factor, S_0^2: amplitude reduction factor and E_0: photoelectron energy for the TiO_2 nanomaterials.

Catalysts	Surface area m^2/g	Pore volume cc/g	Pore width (nm)	Particle size (nm)
C-TiO_2	14.243	0.020	3.537	54
Zn-TiO_{2-x}	247.925	0.335	5.682	12
Mg-TiO_{2-x}	342.598	0.466	5.682	10
AA-TiO_{2-x}	145.654	0.228	5.682	24
CA-TiO_{2-x}	228.254	0.332	4.887	10

Table S. II. The textural properties of all nanocatalysts.

Samples	Band gap (eV)	Valence band edge (eV)	Conduction band edge (eV)
C-TiO_2	3.01	2.91	-0.29
Zn-R-TiO_{2-x}	2.81	2.71	-0.04
Mg-R-TiO_{2-x}	2.66	2.66	-0.04
AA-R-TiO_{2-x}	<1.5	-	-

CA-R-TiO_{2-x}	2.71	2.66	-0.04

Table S.III. Absorption and TRPL data of the synthesized photocatalysts.

Catalysts	**(HER) η @ 10 mA cm^{-2}**	**(OER) η @ 10 mA cm^{-2}**	**Tafel slope (OER) (mV dec^{-1})**	**R_{ct} (Ω)**	**R_s (Ω)**	**CPE or Y^0 (µf)**	**A Surface roughness**	**Wd or R_w (µΩ)**
C-TiO_2	>1000	>1000	181	210.4	22.59	$2.663e^{-6}$	$919.8e^{-3}$	$237.8e^{-6}$
Zn-TiO_{2-x}	750	480	70	10.58	28.20	$7.450e^{-6}$	1.000	$3.807e^{-3}$
Mg-TiO_{2-x}	650	420	62	6.662	18.10	559.6e-6	820.00	$25.97e^{-3}$
AA-TiO_{2-x}	780	485	79	21.75	32.07	$55.21e^{-6}$	$8445e^{-3}$	$4.311e^{-3}$
CA-TiO_{2-x}	790	493	80	12.26	28.10	$999.0e^{-6}$	$870.0e^{-3}$	$25.97e^{-3}$

[a]The electrolyte is 0.1 M NaOH solution.

Table S. IV. Overpotential (HER & OER), Tafel slope and electrochemical impedance data of as prepared electrocatalysts[a].

Electrocatalysts	Current density (j mA cm^{-2})	Overpotential (η/mv)
TiO_2 Zn-TiO_{2-x} Mg-TiO_{2-x} AA-TiO_{2-x} CA-TiO_{2-x}	10	>1000 [Present Work] 750 650 780 790
TiO_{2-x} $TiO_{1.51}$ $TiO_{0.89}$ $TiO_{1.23}$	10	730 [5] 590 340 280
Tour-MWCNTs@Pd/TiO_2 Ox-MWCNTs@ Pd/TiO_2	1	350 [6] 310
TiO_2 (Defect rich titania with 1-7min cathodization)	1	800 [7] 390 370

TABLE S. V : Comparison of overpotential (HER) of present work with few similar works.

REFERENCES

[1] B. Ravel, M. Newville, ATHENA, ARTEMIS, HEPHAESTUS: data analysis for X-ray absorption spectroscopy using IFEFFIT, Journal of Synchrotron Radiation. 12 (2005) 537–541.

[2] S. Gul, J.K. Cooper, P.-A. Glans, J. Guo, V.K. Yachandra, J. Yano, J.Z. Zhang, Effect of Al3+ co-doping on the dopant local structure, optical properties, and exciton dynamics in Cu+-doped ZnSe nanocrystals, ACS Nano. 7 (2013) 8680–8692.

[3] A. Bashir, F. Bashir, Z. Mehmood, M.S. Satti, Z. Akhter, Synthesis, characterisation and investigation of enhanced photocatalytic activity of Sm+ 3, Ni+ 2 co-doped TiO2 nanoparticles on the degradation of azo dyes in visible region, International Journal of Nanoparticles. 11 (2019) 37–61.

[4] W. Chen, G.-R. Duan, T.-Y. Liu, S.-M. Chen, X.-H. Liu, Fabrication of Bi2MoO6 nanoplates hybridized with g-C3N4 nanosheets as highly efficient visible light responsive heterojunction photocatalysts for Rhodamine B degradation, Materials Science in Semiconductor Processing. 35 (2015) 45–54.

[5] Valenti, G., Boni, A., Melchionna, M., Cargnello, M., Nasi, L., Bertoni, G., Gorte, R.J., Marcaccio, M., Rapino, S., Bonchio, M. and Fornasiero, P., 2016. Co-axial heterostructures integrating palladium/titanium dioxide with carbon nanotubes for efficient electrocatalytic hydrogen evolution. *Nature communications*, *7*(1), p.13549.

[6] Swaminathan, J. and Ravichandran, S., 2018. Insights into the electrocatalytic behavior of defect-centered reduced titania (TiO1. 23). *The Journal of Physical Chemistry C*, *122*(3), pp.1670-1680.

[7] Kumar, M.P., Murugadoss, G., Mangalaraja, R.V., Arunachalam, P., Kumar, M.R., Hartley, U.W., Salla, S., Rajabathar, J., ALOthman, Z.A. and ALTalhi, T., 2021. Design and development of defect rich titania nanostructure for efficient electrocatalyst for hydrogen evolution reaction in an acidic electrolyte. *journal of materials research and technology*, *14*, pp.2739-2750.